Deep ultraviolet Raman spectroscopy: A resonance-absorption trade-off illustrated by diluted liquid benzene

C. T. Chadwick, A. H. Willitsford, C. R. Philbrick, and H. D. Hallen

Deep ultraviolet Raman spectroscopy: A resonance-absorption trade-off illustrated by diluted liquid benzene

C. T. Chadwick,[1] A. H. Willitsford,[2,a)] C. R. Philbrick,[1] and H. D. Hallen[1,b)]

[1]*Department of Physics, North Carolina State University, 2401 Stinson Drive, Raleigh, North Carolina 27695, USA*
[2]*John's Hopkins University Applied Physics Lab, 11100 John's Hopkins Rd. Laurel, Maryland 20723, USA*

The magnitude of resonance Raman intensity, in terms of the real signal level measured on-resonance compared to the signal level measured off-resonance for the same sample, is investigated using a tunable laser source. Resonance Raman enhancements, occurring as the excitation energy is tuned through ultraviolet absorption lines, are used to examine the $1332 \, \mathrm{cm}^{-1}$ vibrational mode of diamond and the $992 \, \mathrm{cm}^{-1}$ ring-breathing mode of benzene. Competition between the wavelength dependent optical absorption and the magnitude of the resonance enhancement is studied using measured signal levels as a function of wavelength. Two system applications are identified where the resonance Raman significantly increases the real signal levels despite the presence of strong absorption: characterization of trace species in laser remote sensing and spectroscopy of the few molecules in the tiny working volumes of near-field optical microscopy. © 2015 AIP Publishing LLC.
[http://dx.doi.org/10.1063/1.4938531]

I. INTRODUCTION

Resonance Raman spectroscopy can provide signal enhancements of several orders of magnitude over that observed with normal Raman scattering on a molecule by molecule cross-section basis.[1–3] Recent work has documented many of the benefits of the resonance Raman technique. Species identification can be greatly improved relative to non-resonant Raman because of the greater specificity resulting from larger signals as the excitation wavelength is tuned and the Raman spectral fingerprint signal is enhanced to levels that rival fluorescence signals.[4–12] Many of the current applications of resonance Raman techniques utilize visible and infrared portions of the spectrum, which limit the type of molecules that can be studied and often limits the studies to pre-resonance, rather than resonant excitation at an absorption line. Ultraviolet light can provide resonances in more materials, in particular, explosives,[13–16] but investigations are hampered by available tunable light sources, possible complications relating to sample damage, and fluorescence interference within the Raman spectrum.[1,8] The deep ultraviolet (DUV) resonance Raman regime escapes fluorescence interference from the species of interest and the matrix materials. There are very few materials that have significant fluorescence emission below 280 nm due to pre-fluorescence electron relaxation.[17] Probing in the DUV region also allows access to a range of potentially interesting electronic absorption features, which may be useful for detecting and measuring small concentrations of molecular species.[8,17–25]

A drawback of probing in the DUV region, not emphasized in previous work, is the typical increase in the broadband absorption of most species. When the excitation wavelength is tuned to an absorption line to excite resonance, the wavelength always lies within an absorbing band that limits the penetration depth into the sample. Additionally, the Raman shifted wavelengths may also occur within the absorption band, so strong absorption may occur both as the excitation light enters and as the signal light exits the sample space. For this reason, the measured Raman signal levels (for the same pump power) of single composition bulk species typically do not increase significantly in the DUV resonance Raman regime. We observe a small-factor difference in the real signal levels for orders of magnitude resonant enhancement in several cases. While resonant Raman scattering cross-sections are larger than in the non-resonant, normal Raman scattering case, the effective number of molecules observed is often reduced to those within a thin surface layer in highly concentrated samples. In this paper, we examine the trade-off between resonance enhancement and absorption to investigate when resonance Raman is beneficial. In particular, we find: (a) resonance enhancement can be obtained in some highly absorbing species where normal Raman signals are very weak, (b) this enhancement permits low numbers of molecules to be probed effectively, benefitting trace concentration measurements and tiny volume sample measurements, and (c) the trade-off between resonance enhancement and absorption determines the utility of resonance Raman enhancements.

Applications of Raman resonance enhancements for remote sensing techniques have generated interest, largely for applications in trace concentration detection using lidar.[26] Pre-resonance enhanced Raman lidar has been used to profile and identify trace atmospheric species (sulfur dioxide, carbon tetrachloride, nitrogen dioxide, and nitrobenzene).[26–29] A recent examination of the use of ultraviolet resonance Raman for stand-off detection of roadside bombs

and improvised explosive devices indicates that the enhancement may be limited by heavy absorption.[30] We present here an investigation of: (1) the limitations imposed by the absorption character of the analyte being probed, (2) how the limitations will modify the signal, and (3) use of diluted solutions to investigate example cases. We begin with results on diamond, in which the real signal level decreases as resonance is approached until a modest increase is observed directly at resonance. This illustrates that although the Raman cross section is enhanced; absorption can still dominate in a uniform solid sample. We then investigate the impact of changing the bulk absorption by diluting a resonant liquid benzene sample with non-absorbing liquid heptane. By plotting the data without and with absorption correction, i.e., as raw data and as the per-molecule cross-section, the nature of the resonance/absorption trade-off is illuminated. These results suggest advantages for the application of this enhancement mechanism for trace concentration measurements of species using lidar and for near-field scanning optical microscopy (NSOM). Previous work on NSOM Raman has shown considerable limitations due to tiny signals that require long signal integration times; these problems have necessitated improvements to the instrument design and stability, which are not necessary in normal NSOM systems.[31,32] Since NSOM Raman yields additional information not obtained with far-field Raman techniques,[33,34] the significant enhancements in signal possible from using resonance Raman are advantageous.[35]

II. EXPERIMENTAL SETUP

Continuously tunable excitation source light is generated from 700 nm to 420 nm utilizing an optical parametric oscillator (OPO) [U-Oplaz OPO BBO-3B (type I, model S)] pumped by the third harmonic of a Nd:YAG laser [Spectra-Physics Quanta Ray INDI-50-10]. The visible signal output of the OPO is then frequency doubled by a second harmonic stage [U-Oplaz OPO BBO-SHG (type I, model S)] to yield continuously tunable output from 355 nm to 210 nm. The average power across this wavelength range is 1 mW. The OPO uses type-I phase matching rendering an average bandwidth of 30 cm^{-1} between 355 nm and 210 nm. The pulse length is 7 ns, with excitation at a 10 Hz repetition rate. The laser beam diameter of 0.8 cm typically provides a peak irradiance of ~0.4 mW/cm^2 for the measurements described in this paper. Maintaining a fluence below ~1 mW/cm^2 corresponds to the useful upper limit as described previously[24,36] and avoids saturation effects. In addition, the self-diffusion of benzene between laser pulses provides an adequate change in the scattering volume from one pulse to the next.[4] The unfocused excitation beam produces the Raman signal, which is collected in a standard 90° scattering arrangement and transferred into a triple stage 0.6 m spectrometer [SPEX Triplemate 1877]. The system resolution is limited by the bandwidth of our OPO laser output.

Sample selection was based on absorption features within our OPO tuning range. Diamond was selected to study the uniform solid sample case where absorption increases dramatically as its band gap energy at approximately 205 nm is approached. Benzene was selected for the liquid dilution tests, because it has several absorption features within our operating range, and it is a good reference material due to significant previous work. Heptane is a good solvent with low absorption in the UV and minimal conflicts with the benzene Raman bands. Toluene and naphthalene were also studied as they are chemically similar and both have higher absorption than benzene (these results are not presented here). Absorption data in vapor-phase benzene by Etzkorn *et al.* provide high-resolution spectra with fine wavelength steps, showing the absorption detail.[37,38] Knowledge of the absorption features is also used to predict the attenuation of the Raman scatter signal exiting the sample. The benzene and toluene samples were liquid-phase and housed in a custom made polytetrafluoroethene container with a sapphire window. The sample holder was arranged in a 90° scattering configuration, with both the incident and collected light passing through the sample holder window.[4] Losses introduced by the spectrometer and detector are estimated to find an overall efficiency of approximately 5%. Measurement errors in wavelengths are ±0.05 nm, relative intensities are ±2.5%, and concentrations are ±0.03%. These errors are small relative to the dimensions of the point labels used in the following plots. Our measurements are divided into three main thrusts: (a) observation of resonance enhancement in a pure sample environment, (b) observation of resonance enhancement in diluted sample environments, and (c) detail investigations when tuning on and off of the resonances.

III. RESULTS AND DISCUSSION

Diamond (rough faceted) is used for the uniform solid sample to be studied as the excitation energy approaches a strong absorption feature. The well-known Stokes shifted line at 1332 cm^{-1} dominates its Raman spectrum. A naive expectation is that an increase in the Raman intensity should be observed as we tune closer to the band gap. Indeed, this is the extrapolation of previous pre-resonance Raman studies with tuned excitation wavelengths.[39,40] Calleja *et al.* observed a mild increase in Raman intensity as the excitation wavelength was tuned from 647 nm to 257 nm.[39] However, we observed the opposite, a decrease below 300 nm as the excitation wavelength more closely approaches the expected resonance, as shown in Fig. 1. The decrease corresponds to the behavior expected from the absorption coefficient,[41] which is also plotted on a scale to show its features. The band gap position is indicated by "A" and corresponds with the location of a small resonant gain; however, the real observed signal is decreased by the large absorption within the solid diamond.

In order to further probe this resonance-absorption tradeoff, the study was continued using benzene diluted in heptane. The liquid phase allows measurements at multiple concentrations to study the Raman scattering signals while reducing effects of absorption within the sample. The high absorption of benzene in the DUV region generally limits probing to a layer thickness of a few hundred nanometers for a pure sample. Conversely, the full sample depths (5 mm–15 mm) can be probed in the visible wavelengths due
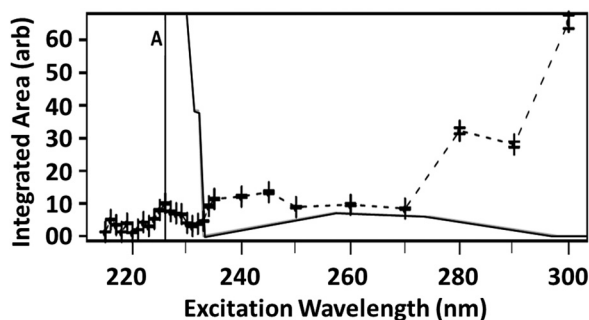
FIG. 1. Points connected by a dashed line show the integrated Stokes Raman relative intensities for the single diamond Raman peak, which is centered at 1332 cm^{-1} as the excitation is tuned from 215 nm to 235 nm in 1 nm steps, and larger steps to 300 nm. The solid line shows the relative absorption coefficient (scaled), from Ref. 40, and the location "A" indicates the band gap edge at approximately 5.5 eV.

to weaker absorption at longer excitation wavelengths. The sampled volume is limited by the collection optics. As we tuned the excitation wavelength ±1 nm over an absorption peak at 258.88 nm in the pure sample case, the typical Raman peak height was approximately 9 times larger at the absorption peak, and clearly marks the resonant enhancement, as shown in Fig. 2.[4,11,12,25] Data from each of the excitation wavelength steps are separated by a scale shift of 0.5 units to separate the curves from each other. The value of this enhancement does not take into consideration the strong self-absorption of the concentrated benzene sample. The remarkable feature is the very narrow line-width dependence of the strong resonance response when the excitation laser is stepped in 1/8 nm increments. In addition, a small wavelength shift indicates stiffening of the interaction as the energy increases. Similar narrow band enhancements are also observed for diluted benzene. While increasing our interaction depth within the sample volume with increased dilution, we still probe only a rather small volume (ranging from several hundred nanometers to a few microns in depth) due to the strong absorption.
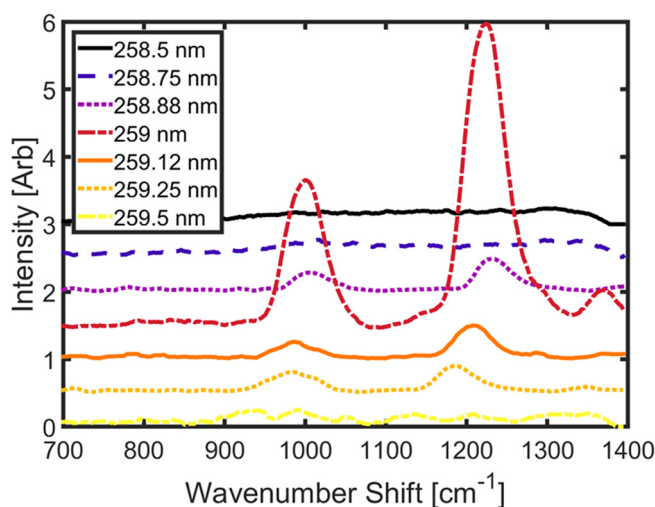

FIG. 2. Stokes Raman spectra for pure liquid benzene (with the wavenumber scale centered at 992 cm^{-1}) as the excitation is tuned from 258.5 nm to 259.5 nm. Resonant Raman gains of several orders of magnitude are seen at 258.88 nm.[4]

Previous work has shown that low concentration environments can be studied using resonance Raman because of the appreciable enhancement yielded as an electronic absorption is approached.[9,42,43] We should emphasize that in those studies, what is typically described as resonance enhancement is actually pre-resonance enhancement. In the present experiments, we have observed the actual resonant behavior, as we have tuned the excitation wavelength across the energy state absorption features. The ∼260 nm benzene absorption line we use shows little pre-resonance, although the higher energy absorption line does produce pre-resonance at these wavelengths.[4,11,12,25]

Figure 3 (top panel) compares the Raman scatter peak area of the 992 cm^{-1} feature at several excitation wavelengths for four different concentrations of benzene dissolved in heptane (v/v is fraction of benzene volume per total solution volume, v/v = 1 represents pure benzene). The data in the top panel of Fig. 3 are only corrected for instrumental and laser tuning effects. These corrections include signal processing to remove background, normalization of the detector quantum efficiency as well as grating and spectrometer throughput efficiency each as functions of wavelength. At the lowest concentrations (2%), the resonant enhancement (at 992 cm^{-1} excited by 259 nm laser) dominates over the non-resonant Raman (excited by 450 nm laser) as the trade-off shifts with sample concentration from being dominated by absorption (100% benzene) to resonance (2% diluted solution). Sample self-absorption and the well-known Raman cross-section frequency dependence (ν^4) are not included. This suggests that when sample concentrations or volumes are small, the resonant enhancements of the Raman scatter should be observable, whereas non-resonant Raman signals are either negligible, masked by fluorescence, dwarfed by the Raman signals from another species, or reduced by the absorption of the ambient background material. As the concentration of benzene is decreased by addition of a non-absorbing material (heptane in this case), the overall absorption decreases, and the Raman signal from the larger volume of non-resonant, heptane, excited molecules becomes comparable to that of the much smaller number of resonantly enhanced benzene molecules. The requirements are no solvent absorption in the excitation band, and minimal overlap of the solvent Raman peaks with those of the trace "sample" species. Then, the enhancement enables access to Raman information in environments where non-resonant Raman signals are too weak due to only trace concentrations of sample species. This result suggests applications in low sample concentration or small volumes such as encountered in NSOM (volumes of order ($\lambda/3$)^3 or less[44,45]), or in LIDAR applications (number densities of species can be ppm to ppt[46]).

Alternatively, Fig. 3 (bottom panel) shows the same data corrected for absorption, giving effectively a per-molecule comparison of Raman cross-section. As expected, the resonant enhancement dominates at all concentrations relative to the non-resonant case (see the ordinate scale, which is in the same arbitrary units for both). Self-absorption of the sample is corrected by multiplication of the ratio of the number of molecules sampled at the visible wavelength
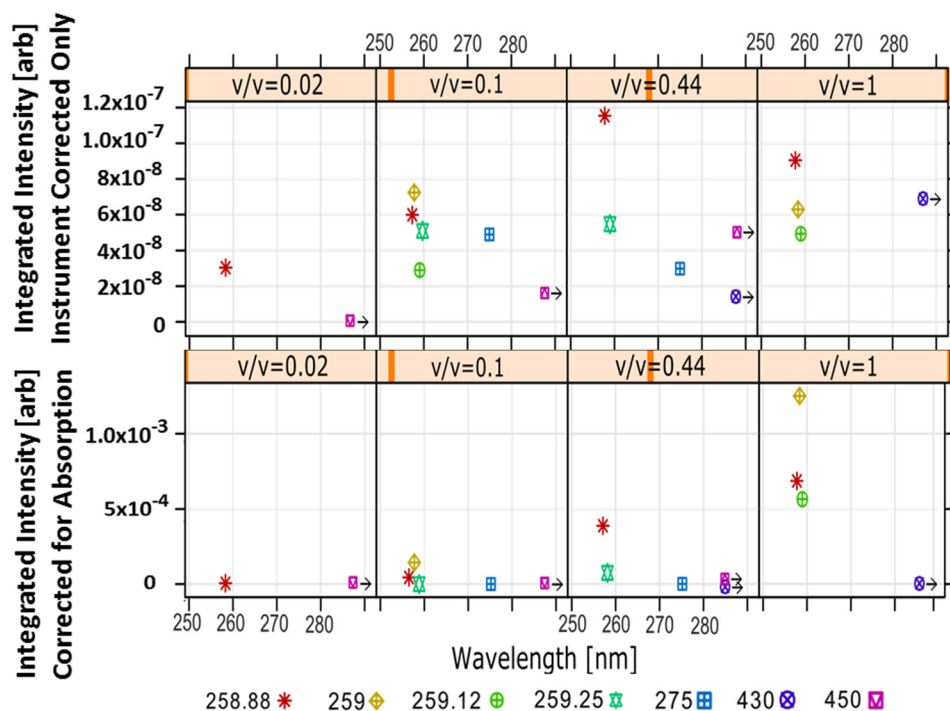
FIG. 3. Two methods are shown to quantify resonance gain. Top panel shows the integrated Stokes Raman intensities for benzene in heptane at various volume concentrations (benzene volume/total volume) and different excitation wavelengths; the data are adjusted only for instrument variation. Bottom panel shows the integrated Stokes intensities corrected for both the instrument variation and for species self-absorption. Both panels use the same arbitrary scale of intensity.

to the number of molecules sampled in the UV. The numerator is calculated using the spectrometer input volume and the denominator by averaging the magnitude of the absorption using Beer's law for both input excitation and output of the Raman-shifted light. This correction includes the fact that the number of visible molecules is limited by the collection volume of the instrument; this factor may have an error ~10%. The volume observed in the UV experiments is limited to a narrow layer next to the viewing window and corresponds to the middle of the spectrometer viewing area, so the error is much less. The details of this calculation can be found in Willitsford *et al.*[4] The magnitude of the corrected signal follows the expected wavelength-dependent cross section times the number of molecules of that species, which increase with concentration, as observed in the figure. The presence of overtone enhancements, the additional species discrimination provided by excitation resonance, and the Raman fingerprint offer further advantages by making use of resonance Raman in either case.

Figure 4 shows another comparison of resonant enhancement. The ratios of the UV to visible Raman signal levels are plotted; again both measured signal levels and absorption-corrected data are shown. When benzene concentrations are high, no significant gains for measured resonance signal levels over those of non-resonant Raman are apparent (ratio values close to unity). However, lower concentrations show very significant enhancements of the measured signal level of resonance over non-resonant Raman signals. While it is not obvious from Figure 3 (bottom panel for 2% benzene case), a resonance gain of approximately 400 times is observed over non-resonant at the absorption peak (258.88 nm, indicated by the up-pointed arrows in Figure 4). When self-absorption is considered, the magnitude is even more pronounced (approximately 48 000 times on a per molecule basis) as shown in the right panel of Figure 4 (note the different ordinate

magnitudes, which use the same arbitrary reference scales). The right panel contains just the enhancement, so a comparison of the two shows the dramatic trade-off between absorption and enhancement; the higher concentration means higher absorption and in turn less enhancement of real measured signals.

A final confirmation of the absorption-resonance trade-off is observed in a highly absorbing species, naphthalene. As previously noted, naphthalene has significantly higher absorption than that of benzene (approximately 30 times that of benzene at the same wavelength). We were unable to obtain any UV Raman signals for different dilute solutions of naphthalene-heptane solutions (as small as 0.003 Molar) or for naphthalene in vapor phase, because of naphthalene's high absorption combined with the effectively smaller number densities. Our conclusion is not that signal enhancement is impossible, but rather there appears to be a diminishing return that depends on the relative intensity of absorption and the inherently low cross-section for Raman vapor-phase signals. We expect some future improvement by utilizing a narrower linewidth excitation source.

The trade-off between high absorption at the excitation wavelength and the resonance Raman signatures can result in significant enhancement of the observed resonance Raman spectra because both are material dependent. Not all materials result in gains in measured resonant Raman signal even at low densities. Also, not all absorption features are useful; for example, the 247 nm and 253 nm absorption lines of benzene yield Raman spectra peaks that are overlapped on the next larger absorption features because of their association with molecular resonance. The more properly chosen 259 nm absorption places the Raman-shifted light in a lower absorption region, where the signal trade-off is favorable.

In this paper, we have not addressed this trade-off from a theoretical point of view. Although beyond the
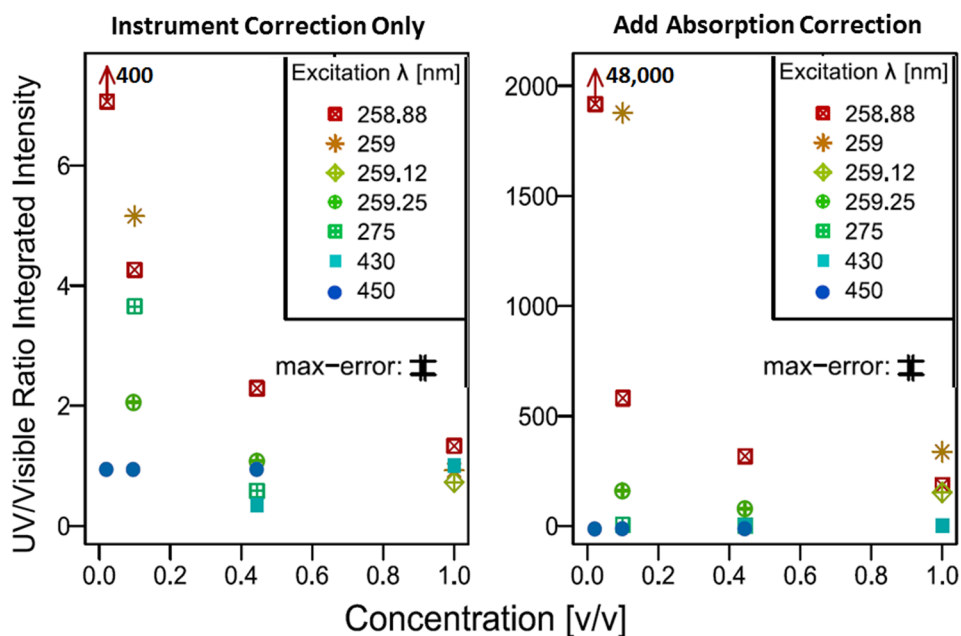
FIG. 4. The ratios of all integrated intensities compared with the non-resonant integrated intensity as a function of concentration are normalized to provide an indication of signal gain. Left panel: the real measured signal gain by adjusting only for the instrument variation—the resonant and visible signals at the pure sample concentrations (v/v = 1) are nearly equal. Right panel: also adjusts for the species self-absorption to compare cross-sections—significant gains are seen when comparing on a per molecule scattering basis. The arrow indicates a point beyond the vertical scale; at the lowest concentration (v/v = 0.02) shows a gain of 400 before the absorption correction, and a value of approximately 48 000 after correction. Both panels are based on the same relative intensity scale.

current, experimentally driven discussion, we note that such a study could be improved upon by considering a time-dependent approach to the calculation of resonant Raman signals[18–20] and by using time-dependent density functional theory (TDDFT) or weighted gradient approximations to improve modeling and simulation efforts for quantum-mechanical pre-resonant and resonant Raman intensity calculations.[47–51]

IV. CONCLUSION

Resonance-Raman scattering in the DUV region has been shown to provide significant cross-section enhancement over non-resonant Raman in species that exhibit high absorption. However, this enhancement may be tempered by signal loss due to strong absorption features responsible for resonance. When the concentration or volume of highly absorbing molecules is large, the measured UV resonance Raman signal may not be significantly larger than non-resonant Raman with visible non-resonant excitation. Different concentrations of benzene dissolved in heptane demonstrate that significant Raman signal enhancements occur as the concentration is reduced, and when the absorption line for excitation is chosen to minimize the absorption of the Raman-shifted signal. Also, we have confirmed the enhancement/absorption trade-off with several species of different absorption characteristics. Enhancements in low sample density environments, such as in trace gas analysis with LIDAR and low sample volumes with NSOM, are expected to provide opportunities for future applications.

[1]A. Kudelski, "Analytical applications of Raman spectroscopy," Talanta **76**(1), 1–8 (2008).
[2]S. A. Asher, "UV resonance Raman spectroscopy for analytical, physical, and biophysical chemistry Part 2," Anal. Chem. **65**(4), 201A–210A (1993).
[3]R. J. H. Clark and T. J. Dines, "Resonance Raman spectroscopy, and its applications to inorganic chemistry," Angew. Chem. Int. Ed. Engl. **25**(2), 131–158 (1986).
[4]A. Willistford, C. T. Chadwick, H. Hallen, S. Kurtz, and C. R. Philbrick, "Resonance enhanced Raman scatter in liquid benzene at vapor-phase absorption peaks," Opt. Express **21**(22), 26150–26161 (2013).
[5]L. Li, S. F. Lim, A. Puretzky, R. Riehn, and H. Hallen, "Near-field enhanced ultraviolet resonance Raman spectroscopy using aluminum bow-tie nano-antenna," Appl. Phys. Lett. **101**(11), 113116 (2012).
[6]H. Hallen, S. Niu, and L. Li, "Time and neighbor interaction in resonance Raman spectroscopy," Proc. SPIE **9198**, 91980F (2014).
[7]H. Hallen, R. R. Neely III, A. Willitsford, C. T. Chadwick, and C. R. Philbrick, "Coherence in UV resonance Raman spectroscopy of liquid benzene and toluene, but not ice," Proc. SPIE **8845**, 884511 (2013).
[8]S. A. Asher and C. R. Johnson, "Raman spectroscopy of a coal liquid shows that fluorescence interference is minimized with ultraviolet excitation," Science **225**(4659), 311–313 (1984).
[9]S. A. Asher, "Ultraviolet resonance Raman spectrometry for detection and speciation of trace polycyclic aromatic hydrocarbons," Anal. Chem. **56**(4), 720–724 (1984).
[10]E. V. Efremov, F. Ariese, and C. Gooijer, "Achievements in resonance Raman spectroscopy: Review of a technique with a distinct analytical chemistry potential," Anal. Chim. Acta **606**(2), 119–134 (2008).
[11]A. H. Willitsford, "Resonance Raman spectroscopy in the ultraviolet using a tunable optical parametric oscillator," Ph.D. thesis, Pennsylvania State University, 2008.
[12]C. T. Chadwick, "Resonance Raman spectroscopy utilizing tunable deep ultraviolet excitation for materials characterization," Ph.D. thesis, North Carolina State University, 2009.
[13]E. D. Emmons, A. Tripathi, J. A. Guicheteau, A. W. Fountain III, and S. D. Christesen, "Ultraviolet resonance Raman spectroscopy of explosives in solution and the solid state," J. Phys. Chem. A. **117**, 4158–4166 (2013).
[14]A. Ehlerding, I. Johansson, S. Wallin, and H. Ostmark, "Resonance-enhanced Raman spectroscopy on explosives vapor at standoff distances," Int. J. Spectrosc. **2012**, 158715.
[15]D. Tuschel, A. V. Mikhonin, B. E. Lemoff, and S. A. Asher, "Deep ultraviolet resonance Raman excitation enables explosives detection," Appl. Spectrosc. **64**(4), 425–432 (2010).
[16]G. Comanescu, C. K. Manka, J. Grun, S. Nikitin, and D. Zabetakis, "Identification of explosives with two-dimensional ultraviolet resonance Raman spectroscopy," Appl. Spectrosc. **62**(8), 833–839 (2008).
[17]A. C. Albrecht, "On the theory of Raman intensities," J. Chem. Phys. **34**, 1476 (1961).

[18]E. J. Heller, R. L. Sundberg, and D. Tannor, "Simple aspects of Raman scattering," J. Chem. Phys. **86**, 1822 (1982).

[19]A. B. Myers, "Resonance Raman intensities and charge-transfer reorganization energies," Chem. Rev. **96**, 911 (1996).

[20]A. Myers Kelley, "Resonance Raman and resonance hyper-Raman intensities: structure and dynamics of molecular excited states in solution," J. Phys. Chem. A. **112**, 11975 (2008).

[21]S. A. Asher, "UV resonance Raman studies of molecular structure and dynamics: Applications in physical and biophysical chemistry," Annu. Rev. Phys. Chem. **39**, 537–588 (1988).

[22]L. D. Ziegler and A. C. Albrecht, "Preresonance Raman scattering of overtones: The scattering of two overtones of benzene in the ultraviolet," J. Raman Spectrosc. **8**(2), 73–80 (1979).

[23]D. P. Gerrity, L. D. Ziegler, P. B. Kelly, R. A. Desiderio, and B. Hudson, "Ultraviolet resonance Raman spectroscopy of benzene vapor with 220–184 nm excitation," J. Chem. Phys. **83**(7), 3209–3213 (1985).

[24]S. A. Asher, C. R. Johnson, and J. Murtaugh, "Development of a new UV resonance Raman spectrometer for the 217–400-nm spectral region," Rev. Sci. Instrum. **54**(12), 1657–1662 (1983).

[25]A. Willitsford, C. T. Chadwick, H. Hallen, and C. R. Philbrick, "Resonance Raman measurements utilizing a deep UV source," Proc SPIE **6950**, 69500A (2008).

[26]H. Rosen, P. Robrish, and O. Chamberlain, "Remote detection of pollutants using resonance Raman scattering," Appl. Opt. **14**(11), 2703–2706 (1975).

[27]C. G. Chen and A. J. Sedlacek III, "Revisiting Raman lidar: application of new techniques to improve system performance," Proc SPIE **2833**, 182–192 (1996).

[28]A. J. Sedlacek, D. Harder, K. P. Leung, P. B. Zuhoski, Jr., D. Burr, and C. L. Chen, "Remote sensing of the atmosphere by resonance Raman lidar," Brookhaven National Laboratory, Optical Society of America, Upton, New York, 1994, bNL–61283.

[29]C. G. Chen, D. L. Heglund, M. D. Ray, D. Harder, R. Dobert, K. P. Leung, M. T. Wu, and A. J. Sedlacek III, "Application of resonance Raman lidar for chemical species identification," Proc SPIE **3065**, 279–285 (1997).

[30]I. Johansson, M. Norrefeldt, A. Pettersson, S. Wallin, and H. Östmark, "Close-range and standoff detection and identification of liquid explosives by means of Raman spectroscopy," in *Detection of Liquid Explosives and Flammable Agents in Connection with Terrorism* (Springer, Netherlands, 2008), pp. 143–153.

[31]C. L. Jahncke, M. A. Paesler, and H. D. Hallen, "Raman imaging with near-field scanning optical microscopy," Appl. Phys. Lett. **67**(17), 2483–2485 (1995).

[32]E. J. Ayars, C. L. Jahncke, M. A. Paesler, and H. D. Hallen, "Fundamental differences between micro- and nano-Raman spectroscopy," J. Microsc. **202**(1), 142–147 (2001).

[33]C. Jahncke and H. Hallen, "Near-field Raman spectra: Surface enhancement, z-polarization, fiber Raman background and Rayleigh scattering," Lasers and Electro-Optics Society Annual Meeting, LEOS 96 (Institute of Electrical and Electronics Engineers, New York, 1996), pp. 176–177.

[34]H. D. Hallen, E. J. Ayars, and C. L. Jahncke, "The effects of probe boundary conditions and propagation on nano-Raman spectroscopy," J. Microsc. **210**(3), 252–254 (2003).

[35]C. L. Jahncke, H. D. Hallen, and M. A. Paesler, "Nano-Raman spectroscopy and imaging with a near-field scanning optical microscope," J. Raman Spectrosc. **27**(8), 579–586 (1996).

[36]S. Asher, "Coal liquefaction process streams characterization and evaluation of uv resonance Raman studies of coal liquid residuals," Report No. DOE/PC/89883-67 (DE93009669) DOE, 1993.

[37]T. Etzkorn, B. Klotz, S. Sørensen, I. V. Patroescu, I. Barnes, K. H. Becker, and U. Platt, "Gas-phase absorption cross sections of 24 monocyclic aromatic hydrocarbons in the UV and IR spectral ranges," Atmos. Environ. **33**, 525–540 (1999).

[38]T. Inagaki, "Absorption spectra of pure liquid benzene in the ultraviolet region," J. Chem. Phys. **57**(6), 2526–2530 (1972).

[39]J. M. Calleja, J. Kuhl, and M. Cardona, "Resonant Raman scattering in diamond," Phys. Rev. B **17**(2), 876–883 (1978).

[40]S. M. Leeds, T. J. Davis, P. W. May, C. D. O. Pickard, and M. N. R. Ashfold, "Use of different excitation wavelengths for the analysis of CVD diamond by laser Raman spectroscopy," Diamond Relat. Mater. **7**(2–5), 233–237 (1998).

[41]D. F. Edwards and H. R. Philipp, "Cubic carbon (diamond)," in *Handbook of Optical Constants of Solids*, edited by E. D. Palik (Academic Press, Inc., Orlando, Florida, 1985); J. H. Callomon, T. M. Dunn, and I. M. Mills, "Rotational analysis of the 2600 Å absorption system of benzene," Philos. Trans. R. Soc. **259**, 499–532 (1966).

[42]C. M. Jones, T. A. Naim, M. Ludwig, J. Murtaugh, P. L. Flaugh, J. M. Dudik, C. R. Johnson, and S. A. Asher, "Analytical applications of ultraviolet resonance Raman spectroscopy," TrAC, Trends Anal. Chem. **4**(3), 75–80 (1985).

[43]S. H. Huerth, M. P. Taylor, H. D. Hallen, and B. H. Moeckly, "Electromigration in YBa$_2$Cu$_3$O$_{7-\delta}$ using a metal clad near-field scanning optical microscope probe," Appl. Phys. Lett. **77**(14), 2127–2129 (2000).

[44]C. L. Jahncke, S. H. Huerth, B. Clark III, and H. D. Hallen, "Dynamics of the tip–sample interaction in near-field scanning optical microscopy and the implications for shear force as an accurate distance measure," Appl. Phys. Lett. **81**(21), 4055–4057 (2002).

[45]R. Toriumi, H. Tai, H. Kuze, and N. Takeuchi, "Tunable solid state UV lidar system for NO monitoring," Proc. SPIE **2833**, 62–69 (1996).

[46]J. Neugebauer and E. J. Baerends, "Combined theoretical and experimental deep-UV resonance Raman studies of substituted pyrenes," J. Phys. Chem. A **109**, 2100 (2005).

[47]J. Guthmuller, "Assessment of TD-DFT and CC2 methods for the calculation of resonance Raman intensities: Application to o-nitrophenol," J. Chem. Theory Comput. **7**, 1082 (2011).

[48]J. Guthmuller, B. Champagne, C. Moucheron, and A. K. De Mesmaeker, "Investigation of the resonance Raman spectra and excitation profiles of a monometallic ruthenium(II) [Ru(bpy)$_2$(HAT)]$^{2+}$ complex by time-dependent density functional theory," J. Phys. Chem. B. **114**, 511 (2010).

[49]A. A. Jarzecki, "Quantum-mechanical calculations of resonance Raman intensities: The weighted-gradient approximation," J. Phys. Chem. A **113**, 2926 (2009).

[50]J. Romanova, V. Liegeois, and B. Champagne, "Resonant Raman spectra of molecules with diradical character: Multiconfigurational wavefunction investigation of neutral viologens," Phys. Chem. Chem. Phys. **16**, 21721 (2014).

[51]V. Barone, J. Bloino, M. Biczysko, and F. Santoro, "Fully integrated approach to computer vibrationally resolved optical spectra: From small molecules to macrosystems," J. Chem. Theory Comput. **5**, 540 (2009).